Jurnal Teknologi

Full Paper

SEMI-BATCH EXPERIMENTAL STUDY ON MULTIPLE CARBON DIOXIDE BUBBLES ABSORPTION IN SWEETENER SOLUTION UNDER VARYING PRESSURES

Ahmed Dheyaa Nsaif*, Ibtehal Kareem Shakir

Baghdad University, College of Engineering, Chemical Engineering Department, IRAQ

Article history
Received
4 January 2024
Received in revised form
23 February 2024
Accepted
8 July 2024
Published Online
17 October 2024

*Corresponding author
ahmed.nasif1507d@coeng.uobaghdad.edu.iq

Graphical abstract

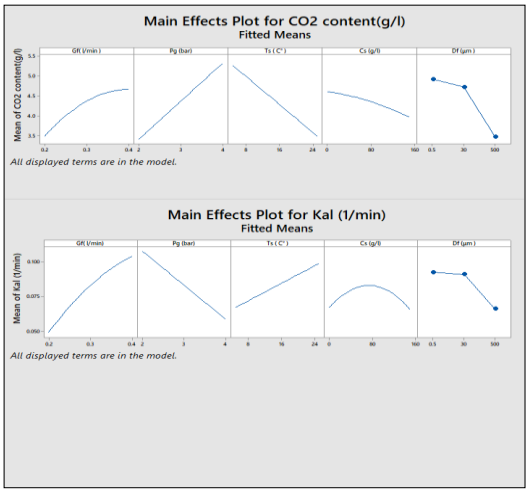

Abstract

Increasing the absorbed carbon dioxide amount in sweetener solution is a new trend to modify soft drinks. This research investigated the optimum increase in absorbed carbon dioxide within the limits of permissible food specifications in the bubble column. Response surface methodology (RSM) utilizing the Box Behnken design (BBD) was used to conduct experiments operating conditions for achieving desired responses within specified ranges of pressure (2-4 bar), temperature (5-25°C), gas flow rate (0.2–0.4 L/min), and absorbent concentration (0–150 g/L). The experimentally obtained results were fitted to a second-order polynomial model—the increase in pressure and gas flow rate results in an increase in absorption yield (Y_{CO2}). Also, increasing the gas flow rate and temperature will increase the volumetric mass transfer coefficient (K_{La}), while, at high pressure and pore size K_{La} will be reduced. According to the obtained results at optimum conditions, 4 bar, 5°C, gas flow rate 0.4 L/min, sucrose concentration of 0 g/L, and pore diffuser 0.5 µm; The CO_2 content (Y_{CO2}) was 8.34 g/L. The optimum conditions for combining the effect of high CO_2 content (6.125 g/L) and best K_{La} value (0.1043 L/min) were: 2.83 bar, 5 °C, a gas flow rate of 0.4 L/min, a sucrose concentration of 65.15 g/L, and pore diffuser of 0.5 µm.

Keywords: Carbon dioxide absorption, Bubble column, Gas diffuser, Volumetric mass transfer coefficients, Box–Behnken design

1.0 INTRODUCTION

The complicated and varied demands of industrial processes necessitate the creation of many types of gas-liquid contactors, including bubble and packed columns [1]. Bubble columns are used a lot in the chemistry industry, especially when there are reactions between different types of gases and liquids, and the liquid phase controls the mass transfer process because gases don't dissolve easily [2]. Since the mass transfer properties (kL and a) are among the most crucial for designing and scaling up bubble columns, they have been the focus of extensive study. Several empirical formulae have been given in the literature for estimating these parameters, and numerous articles contain experimental mass transfer data [3, 4, 5]. Laboratory measurements of volumetric mass transfer coefficients, or interfacial areas, are important. Bubble

size, shape, terminal velocity, and fluid density and viscosity in both stages All of the above variables affect bubble terminal velocity, according to the Stocks equation. Therefore, it affects the dissolved CO_2 content and the volumetric mass transfer coefficient [6, 7, 8, 9]. On the other hand, many scientists are presently researching carbon dioxide capture and storage as a viable strategy for mitigating global warming. Consequently, the investigation of the volumetric mass transfer coefficient of CO_2 assumes significant importance [10, 11]. Although industrial bubble columns are often operated at pressures above atmospheric, almost all of these papers are based on data collected at atmospheric pressure. In the design of gas-liquid reactors operated under pressure, it is imperative to consider the influence of pressure on the variation of kLa. Even so, since there aren't many changes in the physical properties of liquids (like density, viscosity, and diffusivity) in the pressure range that was looked at, it is important to find out why kLa drops as pressure rises, assuming that it does change. On the other hand, the effect of pressure on the liquid-phase mass transfer coefficient kLa has only been the subject of a limited number of published publications [12].

The use of theoretical models alone is inadequate for accurately predicting mass transfer coefficients. Therefore, laboratory-based calculations are conducted under specified operating and design conditions to provide more reliable results. The laboratory behavior of mass transfer exhibits similar characteristics to industrial behavior, given that the operating and design conditions remain consistent. The volumetric mass transfer coefficient is equivalent in both cases [13].

The influence of pressure on mass transfer coefficients for the elements helium (He), hydrogen (Hz), argon (Ar), carbon dioxide (CO_2), and nitrogen (N_2) were introduced into the water for absorption. Additionally, helium (He) and nitrogen (N_2) were absorbed into ethanol and were studied experimentally in a stirred vessel at pressures between 2 and 100 atm [12].

The semi-continuous flow reactor studied CO_2 absorption in aqueous ammonia solutions. This study employed purified CO_2 to eliminate other gases. Solution CO_2 loading and absorption depend on ammonia content, CO_2 inlet velocity, and temperature. Additives affect ammonia's absorption and ammonia loss rate [14].

Physical absorption was studied in continuous and batch modes using a bubble column to measure liquid-phase volumetric mass transfer coefficients (kLa) and absorbent solution viscosity. Process factors included liquid density and viscosity, gas diffusivity and solubility, gas flow rate, pore diameter, and liquid flow rate. Two flow regime-dependent equations link experimental data. Both equations match experimental data by 10% [15].

Experiments were used to study the mass transfer coefficient for CO_2. Several process variables that affect the mass transfer coefficient were changed in a planned way. This included pressure, bubble size, the presence or absence of an inline mixer, retention time, and the type of solvent used [16].

A bubble column batch study examined CO_2 absorption by sucrose and surfactant aqueous solutions. Volumetric mass transfer coefficients (kLa) were calculated for solutions and gas rate flow and associated with superficial gas velocity and liquid phase parameters. Experimental kLa is reproduced by the proposed equation within 10% [17].

From 0.1 MPa to 15 MPa, gas bubble properties in a 5 cm bubble column with a single orifice (1, 3, or 5 mm) were studied. The system pressure significantly impacts gas bubble formation. Under high pressures, a gas jet formed at velocities where spherical bubbles would have formed at atmospheric pressure [18].

The important gas speed between the bubbling and jetting modes was connected to the Weber number in the liquid phase and the Reynolds number in the gas phase, which depended on the speed of the gas moving through the orifice. The distributor's bubble creation pattern had an impact on bubble size and gas holdup in the main bubble column [19].

Air, CO_2, water, and NaOH were used to calculate Kla at 0.1 m column diameter. A gas dispenser with 79 holes with 2 mm-diameter slots is for experimentation. The mass transfer coefficient was predicted using empirical and ANN correlations in dimensionless groups (Sh, Re, Bo, and We) [20].

The volumetric liquid phase mass transfer coefficient, kLa, was determined experimentally in bubble columns with 10 and 19-cm inner diameters. The columns were equipped with single-nozzle gas spargers. The study involved several gases, including air, CO_2, O_2, H_2, and CH_4, as well as various pure liquids (water) and aqueous nonelectrolyte solutions (water + scouse, water + methanol). The investigation aimed to examine the influence of the physical properties of the gas and liquid on the kLa value [4].

CO_2 absorption by a potassium hydroxide aqueous solution was examined. The response surface methodology (RSM) based on central composite design (CCD) was used to design experiments, create models, and determine optimal operating conditions for desired responses at 25–65 °C, 2–10 bar, and 0.01–1.21 mol/L. The effects of process factors and interactions on responses were analyzed using a numerical model based on experimental data and a second-order polynomial model to determine optimal conditions [21].

A batch-packed bed distillation column study uses binary systems: ethanol-water, methanol-water, methanol-ethanol, benzene-hexane, and benzene-toluene. Multiple regression analysis correlates the mass transfer coefficients of the vapor and liquid phases (KOV and KOL) [22].

A simulated feed gas of carbon dioxide and nitrogen was balanced to 1 atmosphere for carbon dioxide capture testing. This study tests monoethanolamide, triethylenetetramine, and diethylenetriamine as poly alkanol amine absorbents. Among the factors affecting performance are amine

inlet concentrations, liquid and gas flow rates, lean amine loading, carbon dioxide concentration at intake, absorbent temperature, and alkanol amine type [23].

The volumetric mass transfer coefficient (Kla) shows a positive correlation with the increase in stirrer speed. The dispersion of bubbles was shown to improve as the speed increased, resulting in an elevated surface-to-volume ratio and mass transfer area (Kla) [24].

This study aimed to find out how different variables (pressure, temperature, gas flow rate, sugar concentration, and the diameter of the pore diffuser) affect the content of CO_2 and the volumetric mass transfer coefficient. Variation in the gas size pores diffuser (0.5 to 500 µm), liquid temperature (5 °C to 25 °C), gas flow rate varying (0.2 to 0.4 l /min), and sucrose concentration (ranging from 0 to 150 g/L). The volumetric mass transfer coefficients are derived from the experimental data. In this study, the Box-Behnken experimental design is employed to conduct statistical analysis. The purpose is to predict the association between the experimental variables and the desired response variables, including the content of CO_2 and the volumetric mass transfer coefficient. These measurements were conducted at both the free gas-liquid interface and the interface between gas bubbles and liquid, within a pressure range of 2-4 bar.

2.0 METHODOLOGY

2.1 Materials

The CO_2 and N_2 gases used in the practical experiments were from Al-Mansour State Company, with a high purity of 99.99%. In addition, the water used in the experiments was RO water from the same company. Food sugar (sucrose, C12H22O11) was used to prepare the solution used in practical experiments. The sample solution was 1.75 liters of RO water plus sucrose.

2.2 Theory

The process of dissolving carbon dioxide in water occurs through the gas-liquid mass transfer phenomenon. To ascertain the rate at which carbon dioxide dissolves, it is important to get a suitable gas-liquid mass transfer coefficient [25].

At the interface between a gas and a liquid, the mass transfer coefficient is an indicator that measures how quickly materials can diffuse and be transported.

The rate of gas absorption per unit time per unit volume of liquid phase (N) can be expressed as:

$$N_{c_{02}} = \frac{dc}{dt} = K_L a\ (C^*_{CO2} - C_{CO2}) \quad (1)$$

The driving force for the transfer process of $C^*_{CO2} - C_{CO2}$ is determined by the disparity between the concentration of the gas in the interface, denoted as C^*_{CO2}, which is in equilibrium with pure gas (also known as solubility), and the concentration of the gas in the bulk liquid. The concentration was assessed by conducting a mass balance analysis of the experimental absorption rates over time. The calculation of the volumetric mass transfer coefficient involves determining the quantity of gas absorbed during a certain period, provided that the volume of the column and the concentrations of the gas at the interface and in the bulk, liquid are known.

2.3 Experimental Setup and Procedures

The experiments were conducted using an experimental configuration, as illustrated in Figures 1 and 2 a, b. The experimental rig consisted of a cylinder of stainless steel 316 with a diameter of 10 cm, a height of 40 cm, and a thickness of 3 mm. It contains a port with a diameter of 0.5 inches at the bottom for entering the feeding gas of CO_2 by connecting a gas diffuser to it.

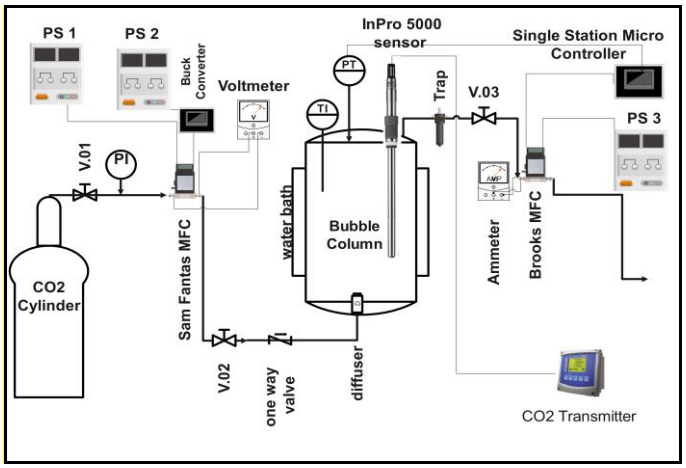

Figure 1 The Schematic Setup of the Sime-Batch Bubble Column CO2-Sweeteners Solution Absorption Atmospheric and under Variable Pressure Systems

At the top, there is a port with a diameter of 0.5 inches for connecting the sensor InPro 5000 with an integrated temperature probe, in addition to a port with a diameter of 6 mm for the exit of CO_2 gas. It's immersed in a water bath to control the internal solution temperature. The water bath is chilled using Freon 134 a, a refrigerant, while the temperature of the water is controlled by a temperature controller type (Hartmann & Braun AG Digitric Z). Two mass flow controllers (MFC), the first (X-TMF, Brooks ®, USA , range 0 – 5 SLPM) and the second (SAM FANTAS, Hitachi, Japan, range 0–0.715 SLPM). It was used to determine and control gas injection flow rate and outlet pressure as a PID controller, stainless steel diffuser (SFHx, HENGKO, China, pore size diameter 0.5–500 µm), It is used in diverse industries to infuse CO_2 gas into a liquid. The purpose is to generate little bubbles or distribute the gas uniformly in the liquid to enhance mixing efficiencyInPro®5000(i) CO_2 Sensors-CO_2 Transmitter 5100 e (Mettler-Toledo, USA) with an integrated temperature probe is used for dissolved carbon dioxide measurement. In addition to the temperature of the liquid, the SINGLE STATION MICRO Plus Controller SSMPC (760, Foxboro, USA) is a microprocessor-driven

device capable of executing PID control functions for two independent loops. A PID controller is used in industrial control systems for controlling pressure. A pressure transmitter (WIKA, Germany, range 0–6 bar) is used to measure pressure and convert it into an electrical signal to control it via a single-station microcontroller. A water trap is used to remove water and other contaminants from the CO_2 gas before it enters the MFC. Electronic Meters The quantity of gas that is fed into the system can be quantified. The voltage output of the MFC can be measured using a voltmeter (DT-9205A), while the gas flow rate outlet can be measured as a current signal using an ammeter (DT-9205VL). There are three power supplies (PS1, PS2, and PS3) for the power source and set point, Buck Converter Its purpose is to regulate and maintain stable voltage levels from the power supply, and all gas ducts are quick-fitting Inline Shut Ball Valves (Turkish), 6 mm outside diameter and 4 mm inside diameter. The experiment utilizes reverse osmosis (RO) water and various concentrations of sucrose as the solution.

Figure 2(a) Photographic picture of apparatus used for semi-batch CO2 absorption system

Figure 2(b) Photographic picture of the system's parts

The solution designated for each experiment was prepared by mixing 1.75-liter RO water with the required amount of sucrose until it was completely dissolved to get different sucrose concentrations then entered into the system. Nitrogen gas was pumped to remove any impurities and dissolving concentrations, as well as distribute the temperature of the solution. MFC must be operated by power supplies PS1 and PS3 for no less than 45 minutes, according to the manufacturer's recommendations, to warm up and stabilize their temperature to ensure the accuracy of measurement.

ize their temperature to ensure the accuracy of measurement.

The cooling system was turned on to reach the desired solution temperature. The temperature is carefully controlled within a tolerance of ± 0.5 degrees Celsius.

Closed the valve for Brooks MFC completely 0.00% and switch the single-station microcontroller to manual mode. And set the gas pressure inside the bubble column as setpoint pressure.CO_2 gas is pumped into the bubble column from the top until it reaches the setpoint pressure for the purpose of reaching a study state as quickly as possible and avoiding fluctuations in the PID controller. At the start of operation, the PT (pressure transmitter) sends the pressure as an analogue signal (4–20 mA) to the single-station microcontroller for the purpose of processing it and comparing it with the setpoint pressure. Then the single-station microcontroller works to send an analogue signal (4–20 mA) to the Brooks MFC for the purpose of opening and closing the valve for the purpose of controlling the pressure. This procedure continues until the solution reaches saturation with CO_2 gas. The valve V.01, V.02, V.03 is opened for the purpose of CO_2 gas flowing from high pressure cylinder at a pressure higher than the experimental pressure of 50 psi. After that, the amount of CO_2 gas flow in the Sam Santa MFC is adjusted using PS2, with a modified and stable voltage, using a Buck Converter because the fluctuation of current and voltage. a Buck converter connected in series with PS2 was used to obtain a constant and stable voltage. The gas flow coming out of the MFC is measured by a voltmeter. The gas flow is constant, and the error rate is approximately 0.05%.

The CO_2 gas passes through the one-way valve to ensure that the liquid does not return from the bubble column to inlet pipe. The gas then passes through the gas diffuser placed inside the tower in the center of the base. The gas then flows through a gas diffuser, which has micro-diameter pores to achieve smaller bubbles undergo dissolution in the solution at a constant temperature

The sweetened liquid is controlled at the temperature chosen in the experiment by means of a water bath cooled by Freon gas and controlled by a temperature controller.

As for Brook MFC, it is set to 100% valve opening using a single-station microcontroller. because the process is under atmospheric pressure and does not require a control system The device is for the purpose of measuring the amount of CO_2. The ammeter is used to measure this amount. The concentration of CO_2 gas

in the solution is measured by a CO_2 sensor, in addition to the difference between the amount of gas entering and exiting during the experiment.

The unabsorbed gas passes from the bubble column through a water trap for the purpose of not contaminating the MFC device. In addition to the accuracy of the CO_2 gas measurement, the amount of unabsorbed CO_2 gas is measured using an ammeter connected to the analogue signal output of the Brooks MFC. The experiment continues until the solution reaches the saturation stage, where the amount of gas entering and leaving the system is equal.

The time for the experiment was considered to be 25 minutes because the minimum experiment time for CO_2 saturation was 25 minutes

The quantity of carbon dioxide (CO_2) assimilated throughout the experimental trials was determined through the use of the subsequent mathematical equation (2):

$$C_{C_{02}}\,Content\ (g/l) = \frac{M_i - M_0}{V_L} \quad (2)$$

where Mi and Mi are the mass flow rate inlet, Mo is the mass flow rate outlet, and V_L is the volume of the water sucrose solution 1.75 liters.

2.4 Response Surface Methodology

The experimental design refers to the optimization of CO_2 absorption in a sweetened solution, specifically focusing on the volumetric mass transfer coefficient. The experiment was conducted via the response surface method (RSM). Response surface methodology (RSM) encompasses a range of statistical and mathematical methodologies that offer notable benefits in the development, enhancement, and optimization of various processes [26].

The contributions of individual and multiple independent variables to processes are better understood with RSM. This experimental methodology not only analyses the impacts of independent variables but also produces an empirical model that characterizes the corresponding quantity of the process [27]. In recent years, response surface methodology (RSM) has been the optimization method of choice. Software (Minitab 18) was used for both the experimental design and statistical analysis. A Box-Behnken (BBD) diagram with three levels and five factors. The total number of experiments was 81 runs. The D-optimality method was chosen to select the 32 observations that gave the best response. Randomizing the order of the experiments helped reduce the impact of random variability in the observed response due to irrelevant factors. Table 1 displays the values for the three continuous independent variables (X1) CO2 pressure (bar), (X2) gas flow rate (l /min), temperature (X3), (X4) sucrose concentration (g/L), and one Categories independent Variable (X5) pore diffuser diameter (µm).

Table 1 Box–Behnken experiment design by Minitab program

Factors	Unit	Symbol	level		
			1	2	3
Pressure (Pg)	bar	X1	2	3	4
Gas flow rate (Gf)	L/min	X2	0.2	0.3	0.4
Temperature (Ts)	°C	X3	5	15	25
Concentration (Cs)	g/L	X4	0	75	150
Diffuser pore diameter (Df)	µm	X5	0.5	30	500

3.0 RESULTS AND DISCUSSION

3.1 RSM Statistical Analysis

The Box-Behnken design was used to investigate the interaction effects of variables such as pressure, temperature, solvent concentration, diameter of pore diffuser, and gas flow rate, which are the primary parameters that affect the absorption process. The CO_2 content and volumetric mass transfer coefficient of CO_2 (as responses) was the variables that were studied after 25 minute. The designed studies utilizing BBD are presented, along with the responses, in Table 2. According to the findings, the content of CO_2 and KLa in the operating conditions ranged from (2.24 – 7.89) g/land (0.0222 – 0.1654) 1/min respectively. These percentages were derived from the data.

Table 2 Experimental design and response values

Run	Gf L/min	Pg bar	Ts C°	Cs g/L	Df µm	CO_2content g/L	KLa 1/min
1	0.2	3	5	75	500	2.89	0.0222
2	0.4	3	25	75	500	3.24	0.0664
3	0.3	2	15	150	500	2.56	0.0598
4	0.3	4	15	0	500	4.60	0.04
5	0.2	3	25	75	500	2.24	0.0352
6	0.3	2	15	0	500	3.3	0.0536
7	0.3	4	25	75	0.5	5.11	0.085
8	0.4	2	15	75	30	3.72	0.1654
9	0.4	3	5	75	500	5.06	0.1001
10	0.3	4	15	150	500	3.61	0.0319
11	0.3	3	25	0	30	3.76	0.0981
12	0.4	3	15	150	0.5	5.13	0.0877
13	0.3	4	5	75	30	7.03	0.0385
14	0.4	4	15	75	30	6.72	0.07
15	0.3	3	25	150	30	3.64	0.1011
16	0.2	2	15	75	30	3.27	0.0748
17	0.3	3	5	0	30	5.89	0.0473
18	0.3	4	25	75	30	5.05	0.074
19	0.3	3	5	150	30	5.95	0.0541
20	0.3	3	15	75	0.5	5.03	0.086
21	0.3	2	25	75	0.5	3.04	0.1578
22	0.4	3	15	0	0.5	5.16	0.0952
23	0.2	3	15	0	0.5	4.24	0.0455
24	0.3	2	5	75	0.5	4.74	0.0937
25	0.3	4	5	75	0.5	7.89	0.0416
26	0.2	3	15	150	0.5	4.23	0.0449
27	0.2	4	15	75	30	4.6	0.0339
28	0.3	3	15	75	500	3.43	0.09
29	0.4	3	15	0	30	5.07	0.1004
30	0.3	2	5	75	30	4.75	0.0794
31	0.3	2	25	75	30	2.88	0.1498
32	0.2	3	15	0	30	4.09	0.0444

By fitting the experimental data to a second-order polynomial model, they underwent analysis. To assess the accuracy of the model and determine its significance, an analysis of variance (ANOVA) was conducted. Tables 3 and 4 present the outcomes of the variance analysis conducted on the suggested response surface quadratic model for CO_2 content and KLa. The model parameters that have P-values below 0.05 and 0.001 are considered significant and highly significant in the model, respectively. Conversely, the model terms with a P-value beyond 0.1 are deemed not significant [28, 29, 30].

Table 3 ANOVA results for the RSM-BBD model of CO_2 content

Source	DF	Adj SS	Adj MS	F-Value	P-value
Model	19	53.8876	2.8362	113.15	0.000
Linear	6	44.7463	7.4577	297.52	0.000
Gf	1	5.0738	5.0738	202.42	0.000
Pg	1	14.3042	14.3042	570.66	0.000
Ts	1	12.3099	12.3099	491.10	0.000
Cs	**1**	0.3346	0.3346	13.35	0.003
Df	2	12.5438	6.2719	250.22	0.000
Square	2	0.7901	0.3951	15.76	0.000
Gf^2	1	0.7190	0.7190	28.68	0.000
Cs^2	1	0.0936	0.0936	3.73	0.077
2-way Interaction	11	3.6529	0.3321	13.25	0.000
G *Pg	1	0.6972	0.6972	27.82	0.000
Gf*Ts	1	0.3422	0.3422	13.65	0.003
Gf*Df	2	0.2313	0.1157	4.61	0.033
Pg*Ts	1	0.1770	0.1770	7.06	0.021
Pg*Df	2	1.1211	0.5606	22.36	0.000
Ts*Df	2	0.6172	0.3086	12.31	0.001
Cs*Df	2	0.4667	0.2334	9.31	0.004
Error	12	0.3008	0.0251		
Total	31	54.1884			

Table 4 ANOVA results for the RSM-BBD model of Kla

Source	DF	Adj SS	Adj MS	F-Value	P-value
Model	15	0.039527	0.002635	34.27	0.000
Linear	6	0.026932	0.004489	58.38	0.000
Gf	1	0.010544	0.010544	137.12	0.000
Pg	1	0.008579	0.008579	111.57	0.000
Ts	1	0.003563	0.003563	46.33	0.000
Cs	1	0.000007	0.000007	0.09	0.765
Df	2	0.004206	0.002103	27.35	0.000
Square	2	0.002469	0.001234	16.05	0.000
Gf^2	1	0.00033	0.00033	4.29	0.055
Cs^2	1	0.002185	0.002185	28.42	0.000
2-way Interaction	7	0.005914	0.000845	10.99	0.000
Gf*Pg	1	0.000743	0.000743	9.66	0.007
Gf*Ts	1	0.000543	0.000543	7.06	0.017
Pg*Ts	1	0.000386	0.000386	5.03	0.04
Pg*Df	2	0.001338	0.000669	8.7	0.003
Ts*Df	2	0.002904	0.001452	18.88	0.000
Error	16	0.00123	0.000077		
Total	31	0.040757			

The P-values for the proposed model terms CO_2 content and KLa were found to be less than 0.0001, as shown in Tables 3 and 4. This indicates that the model terms are highly significant. A large F value suggests that the regression equation explains most of the response variation. The F value of 113.15 in the ANOVA for CO_2 content indicates a substantial effect of the model terms on the response. The model produces R2 99.44% and adjusted R2 98.57%. This means that the proposed model cannot explain at least 0.56 % of experimental outcomes. A chance of $p < 0.05$ exists.

At 95% probability, the model terms are significant. Factors or interactions with $p < 0.05$ are significant. R2 = 95.92, as predicted, indicates that the present model has a significant block effect. A value of (predicted R2 −adjusted R2) < ± 0.20, indicates either no problem with the data or the model. indicates either no problem with the data or the model. similarity, The ANOVA analysis reveals that the F value of 34.27 for KLa shows a significant impact of the model terms on the response variable. The model has an R-squared value of 96.98% and an adjusted R-squared value of 94.15%. This implies that the proposed model is unable to account for a minimum of 3.02 % of observed experimental results. There is a probability of $p < 0.05$. The model terms exhibit significance at a confidence level of 95%. Significant factors or interactions are those with a p-value less than 0.05. The obtained R2 value of 91.62% aligns with the predicted outcome, providing evidence that the current model exhibits a substantial block effect. A discrepancy of (predicted R2 − adjusted R2) within the range of < ± 0.20 suggests that there is either no problem with the data or the model [26].

Finally, the Box-Behnken Design-determined regression model equation is defined as (3,4,5,6,7and 8) in terms of experimental variables (with a confidence level of 95% or higher).

Based on Figure 3 a.b for the content of CO_2 and KLa, it is evident that the residuals exhibit a normal distribution. This conclusion can be inferred by visually assessing the plotted data points and their corresponding values. In the normal probability plot, a significant number of points are observed to be near the line. Conversely, in the fitted value form, the points lack a distinct shape. The data points are distributed randomly and can be observed in the histogram. The presence of a vertex indicates that the data set has a single mode, which is commonly referred to as unimodal. Additionally, the data points are arranged in ascending order, with no outliers present within the range [29].

Df	CO_2 Content	
o.5	= 01.000 +12.67 Gf + 0.159 Pg + 0.0197 - 0.00018 Cs - 28.58 Gf2- 0.000016 Cs2+ 4.350 Gf*Pg) - 0.2800 Gf*Ts - 0.01425 Pg*Ts	3
30	=1.022 +13.80 Gf- 0.059 Pg + 0.0275 Ts - 0.00052 Cs - 28.58 Gf2 - 0.000016 Cs2 + 4.350 Gf*Pg - 0.2800 Gf*Ts - 0.01425 Pg*Ts	4
500	=-0.26 +18.21 Gf- 0.442 Pg + 0.0706 Ts- 0.00281 Cs - 30.70 Gf2- 0.000020 Cs2+ 4.175 Gf*Pg- 0.2925 Gf*Ts - 0.01487 Pg*Ts	5
	Kla	
0.5	=-0.2177+1.249 Gf+ 0.0201 Pg+ 0.00827 Ts+ 0.000437 Cs- 0.652 Gf2- 0.000003 Cs2- 0.1363 Gf*Pg- 0.01165 Gf*Ts- 0.000695 Pg*Ts	6
30	=-0.2160 +1.249 Gf+ 0.0197 Pg+ 0.00813 Ts+ 0.000437 Cs- 0.652 Gf2- 0.000003 Cs2- 0.1363 Gf*Pg - 0.01165 Gf*Ts- 0.000695 Pg*Ts	7
500	=-0.2587 +1.249 Gf+ 0.0409 Pg+ 0.00507 Ts+ 0.000437 Cs- 0.652 Gf2- 0.000003 Cs2- 0.1363 Gf*Pg - 0.01165 Gf*Ts- 0.000695 Pg*Ts	8

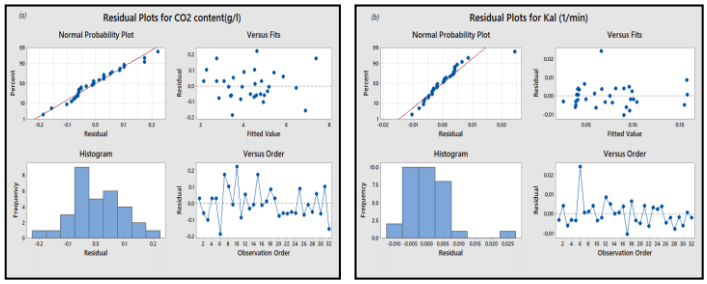

Figure 3 Residual plots (a) CO_2 content (g/L), (b) KLa (1/min)

The residuals exhibited a distribution near the straight line, indicating a satisfactory relationship between the experimental and predicted values of the response This relationship can be observed in Figure 4 a b.

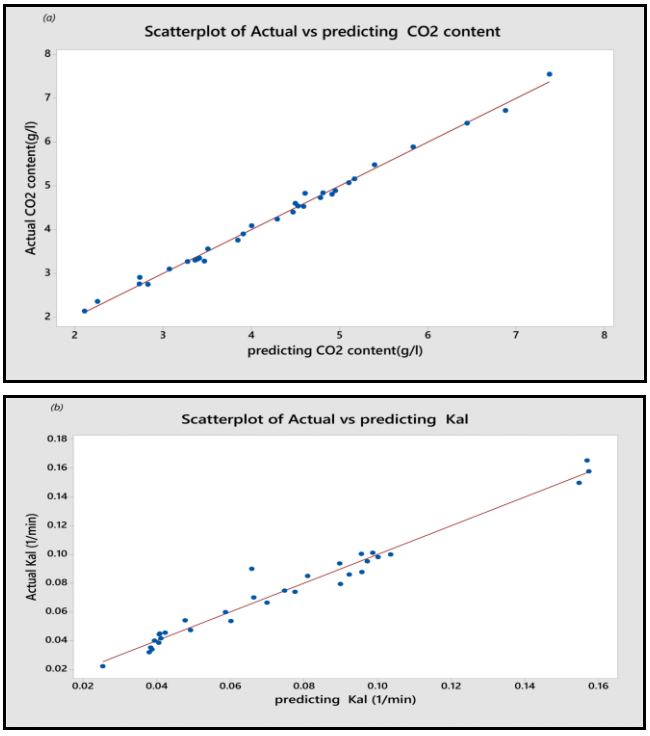

Figure 4 Actual vs predicting (a) content CO_2 (g/L) (b) KLa (1/min)

The main effect plots of experimental parameters (X1, X2,X3,X4 and X5) the content of CO_2 and Kla were shown in Figure 5 and 6 respectively . The Main Effects Plot for CO_2 content(g/l) increased with increased pressure and gas flow rate and decreased with increased temperature, concentration and pore size diameter. as well as The Main Effects Plot for Kla (1/min) increased with increased temperature and gas flow rate and decreased with increased pressure and pore size diameter excepted the midst value of concentration given maximum main effect of Kla.

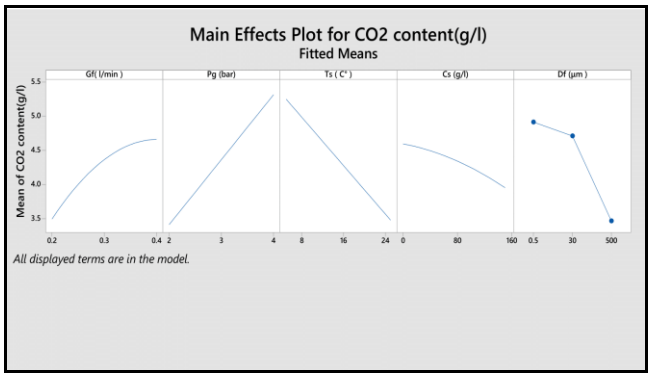

Figure 5 main effects of plot for CO_2 content

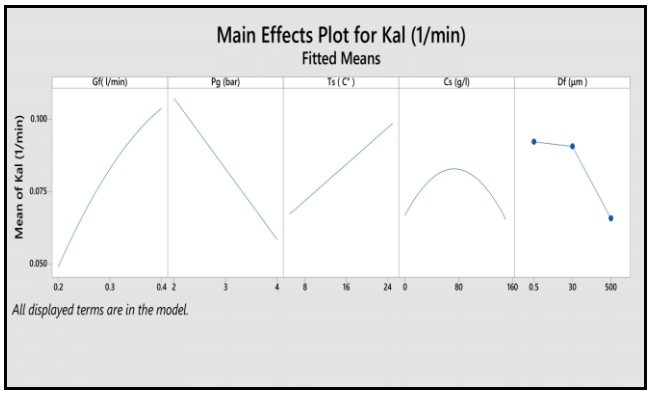

Figure 6 main effects of plot for CO_2 Kla

3.2 Effects of Operating Conditions

To enhance the comparability of the impacts of the operational parameters, supplementary experiments were conducted alongside the specified trials utilizing the Box-Behnken design. These additional experiments are documented in Table 3. The present study examines the influence of pressure, temperature, gas flow rate, source concentration, and pore diffuser diameter on the CO_2 content. This investigation is conducted by analyzing a series of tests, including those outlined in Table 2.

Table 5 Additional Experimental design and response values

Run	Gf L/min	Pg bar	Ts C°	Cs g/L	Df µm	CO_2content g/L	KLa 1/min
1	0.3	4	15	75	30	10.48	0.055
2	0.6	4	25	75	30	12.98	0.123
3	0.4	3	15	75	30	9.95	0.1055
4	0.4	5	15	75	30	13.88	0.057
5	0.3	4	15	75	0.5	10.94	0.0515
6	0.3	4	35	75	0.5	7.11	0.1045
7	0.4	3	15	75	0.5	9.95	0.1095
8	0.4	4	15	225	0.5	9.55	0.1151
9	0.2	3	15	0	500	4.92	0.0383

3.2.1 Effect of Pressure

CO_2 content during absorption is summarized as a function of absorption process time in Figure 7 under the following conditions: 75 g/l absorbent concentration, 15 °C temperature, 0.4 l L/min gas flow rate, 30 mm pore diffuser diameter, 2, 3, and 4 bar pressures as expected, with increasing pressure, the CO_2 content increased. Boosting the driving force of mass transfer due to an increase in CO_2 partial pressure leads to a rise in CO_2 concentration [31].

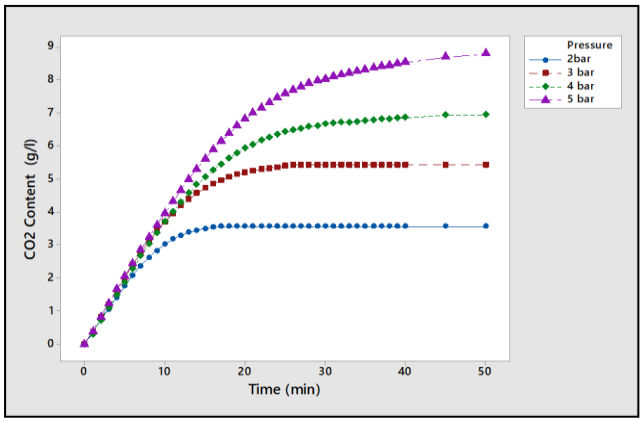

Figure 7 Experimental CO_2 content by water sucrose solution at a sucrose concentration of 75 g/L, the temperature of 15 °C, gas flow rate 0.4 L/min, diffuser pore diameter 30 µm, and pressures of 2, 3, 4and 5 bar

3.2.2 Effect of Temperature

Temperature effects on CO_2 content during absorption of 75 g/L of sucrose aqueous solution at 4 bar and 0.4 L/min of gas flow rate and 30 µm pore diameter of the diffuser are shown in Figure 8. As can be observed, the equilibrium CO_2 content was greatest at 5°C, and as the temperature was raised, the CO_2 loading in equilibrium decreased. by the principle of Henry's Law. Henry's Law states that the solubility of a gas in a liquid is inversely proportional to the temperature of the system. In the case of CO_2, as the temperature rises, the solubility of CO_2 in water decreases. Kinetic energy increases with higher temperatures, explaining these declines. Gas molecules' greater kinetic energy makes them move faster and reduces intermolecular cohesive forces, lowering surface tension and allowing them to break bonds and escape the solution [31, 32, 33].

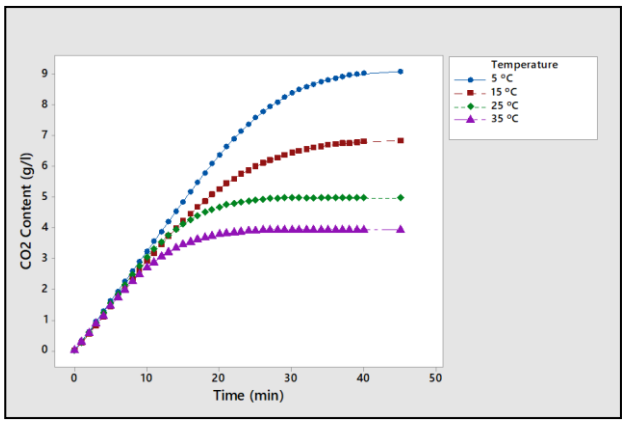

Figure 8 Experimental CO_2 content by water sucrose solution at a sucrose concentration of 75 g/L, the pressure of 4 bar, gas flow rate 0.3 L/min, diffuser pore diameter 0.5 µm and absorbent temperature of 5, 15, 25and 35°C

3.2.3 Effect of Gas Flow Rate

The relationship between the flow rate of CO_2 gas (L/min) and the content of CO_2 measured in g/L is depicted in Figure 9. The graph illustrates an increasing pattern of carbon dioxide concentration with increasing gas flow rate, which can range from 0.2 to 0.4 (L/min). These results were consistent with studies on carbon dioxide absorption.

The increase in the gas flow rate resulted in an improvement in the efficiency of the absorption process. The increase in the rate of gas flow improved the liquid phase mixing, which in turn led to an increase in the specific surface area, which in turn led to an increase in the rate of gas–liquid mass transfer, which in turn led to an improvement in the rate at which CO_2 was absorbed [34, 35, 36].

3.2.4 Effect of the Bubble Size

Figure 10 compares the CO_2 content according to the diameter of the pore diffuser in RO water at a pressure of 3 bar, a flow rate of 0.2 L/min, and a temperature of 15°C. The presented figure illustrates an opposite relationship between the carbon dioxide content and the size of the bubbles, wherein an increase in the content corresponds to a decrease in bubble size. The increase in CO_2 content is due to A smaller decrease in bubble size leads to an increase in the quantity of bubbles, while an enlargement in the contact area between the bubble and solvent occurs. These results were consistent with studies on carbon dioxide absorption and volumetric mass transfer coefficient. [16].

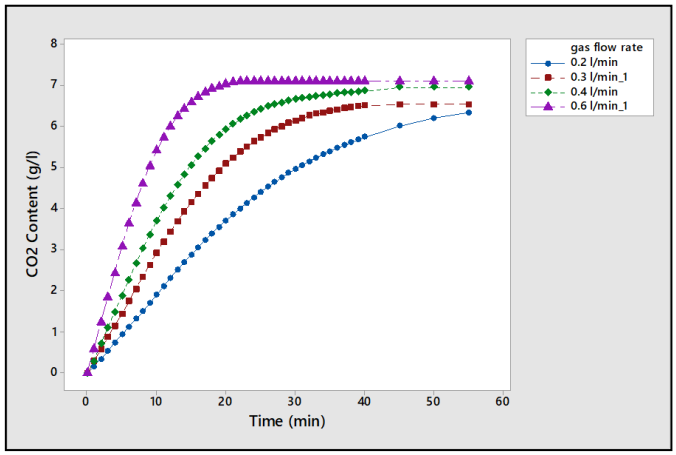

Figure 9 Experimental CO_2 content by water sucrose solution at a sucrose concentration of 75 g/L, the pressure of 4 bar, absorbent temperature of 15 °C, diffuser pore diameter 30 µm and gas flow rate of 0.2, 0.3, 0.4, and 0.6 L/min

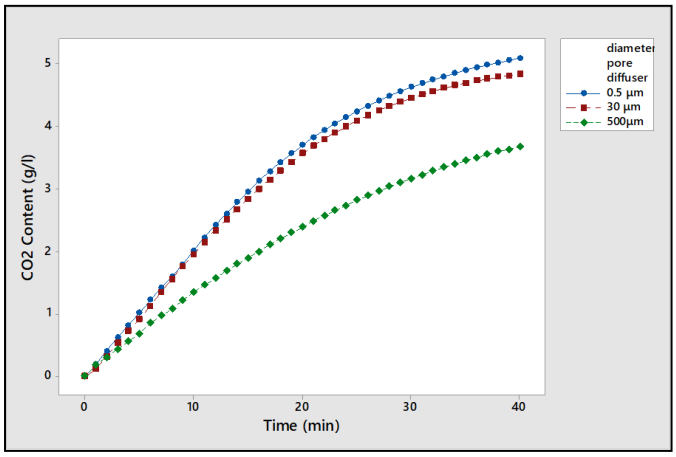

Figure 10 Experimental CO_2 content by Ro water, the pressure of 3 bar, absorbent temperature 15 °C, the gas flow rate of 0.2 L/min. and diffuser pore diameters 0.5, 30, and 500 µm

3.2.4 *Effect of Sucrose Concentration*

The results obtained with three different samples are displayed in Figure 11; all of the samples had the same operating conditions (temperature of 15 degrees Celsius, pressure of 3 bars, diameter of pore diffuser 0.5 µm and gas flow rate of 0.3 L/min, but the sugar concentrations of the samples (0, 75 and 150 g/L). There is a difference in the CO_2 content of each of the samples. When there is a rise in the total amount of sugar present, there is a corresponding drop in the average amount of dissolved carbon dioxide. These results were consistent with studies on carbon dioxide absorption and volumetric mass transfer coefficient [32].

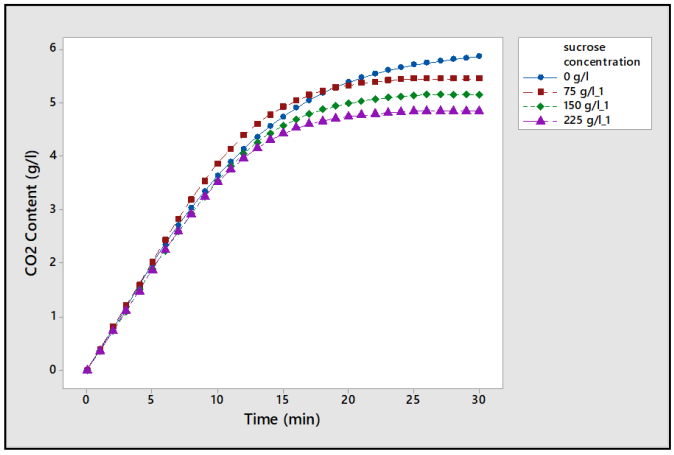

Figure 11 Experimental CO_2 content by Ro water, the pressure of 3 bar, absorbent temperature 15 °C, gas flow rate of 0.4 L/min., diffuser pore diameter 0.5 µm and sucrose concentration of 0,75,150 and 225 g/L.

4.3 Operating Parameter Interactions

In this study, a methodology involving the utilization of contour plots was employed to investigate the interdependent interactions between the operational parameters and responses. The objective was to gain a comprehensive understanding of the interacting dynamics between these variables. To determine the optimal operating parameters for attaining the user express a request for specific responses. All relationships studied were under the following operational conditions pressure 3 bar, temperature 15 °C, gas flow rate 0.3 L/min, sucrose concentration 75 g/L, and diameter of pore diffuser 30 µm.

4.3.1 *Effect of Interaction Variables on CO_2 Content*

Contour plots were employed to investigate the interdependent relationships between the operating parameters and responses, to identify the optimal operating conditions necessary to get the desired responses. The content of CO_2 is shown in Figure 12 as a function of both the temperature and the pressure. Both an increase in pressure and a decrease in temperature have a beneficial impact on the amount of CO_2 content, it can be seen that the effects of both parameters of temperature and pressure in the investigated range are almost the same.[37], [38].

The amount of CO_2 that is present can be shown to be a function of both the pressure and the flow rate of the gas in Figure 13. The amount of CO_2 that is present can be seen to be at its highest when both the pressure and the flow rate are at their highest. The influence of pressure on CO_2 content is slightly higher than the effect of gas flow rate on CO_2 content.

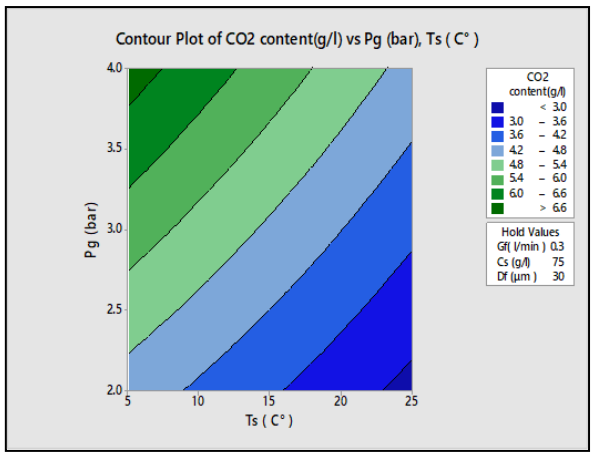

Figure 12 Contour plots Pressure and Temperature

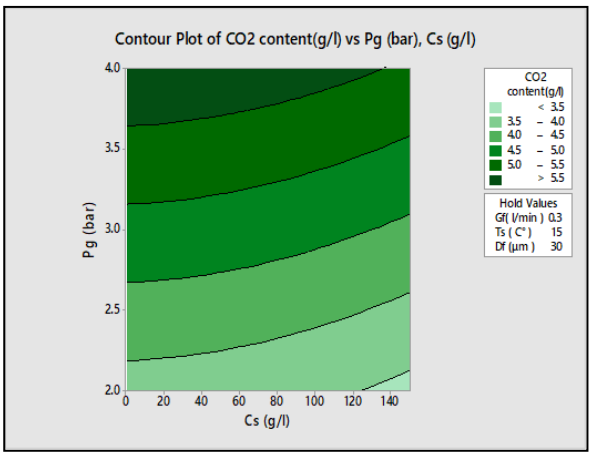

Figure 14 Contour plots Pressure and sucrose Concentration

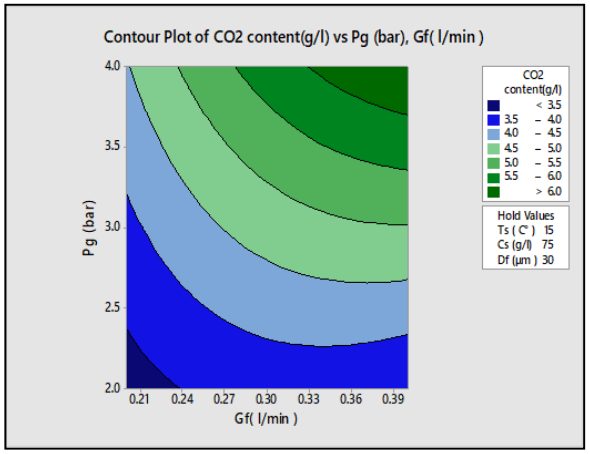

Figure 13 Contour of sucrose Concentration and Temperature

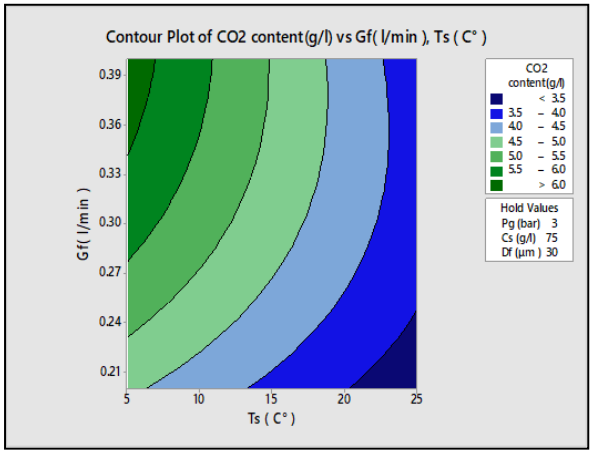

Figure 15 Contour plots Temperature and Gas flow rate

According to Figure 14, which depicts the amount of CO_2 present about the pressure and the concentration of sucrose, the amount of CO_2 present is highest when the pressure is the highest and the sucrose concentration is the lowest [38, 39].

The content of CO_2 that is present can be shown to be a function of both the temperature and the flow rate of the gas in Figure 15. The amount of CO_2 that is present can be seen to be at its highest when the gas flow rate is the highest and the temperature is the lowest.

According to Figure 16, which depicts the content of CO_2 present at the gas flow rate and the concentration of sucrose, the content of CO_2 present is highest when the gas flow rate is the highest and the sucrose concentration is the lowest.

The content of CO_2 that is present can be shown to be a function of both the temperature and the sucrose concentration in Figure 17. The content of CO_2 that is present can be seen to be at its highest when the temperature is the lowest and the sucrose concentration is the lowest.

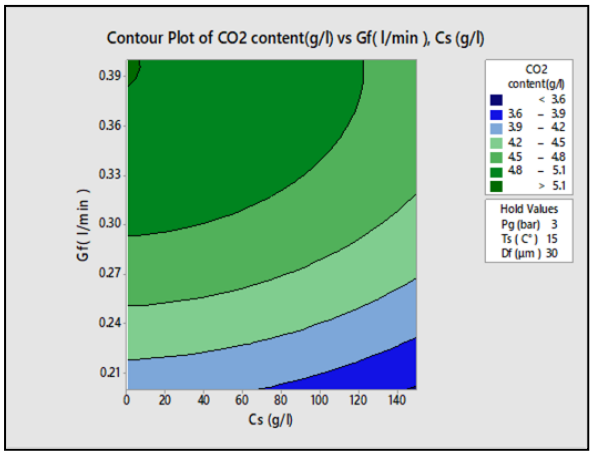

Figure 16 Contour of sucrose Concentration and Temperature

4.3.2 *Effect of Interaction Variables on KLa*

Contour plots were employed to investigate the interdependent relationships between the operating parameters and responses, to identify the optimal operating conditions necessary to get the desired

responses. The KLa of CO_2 is shown in Figure 18 as a function of both the temperature and the pressure. Both an increase in pressure and a decrease in temperature have a decrease on the KLa [40].

The KLa of CO_2 that is present can be shown to be a function of both the pressure and the flow rate of the gas in Figure 19. The KLa of CO_2 that is present can be seen to be at its highest when the pressure is lowest and the flow rate is at its highest.

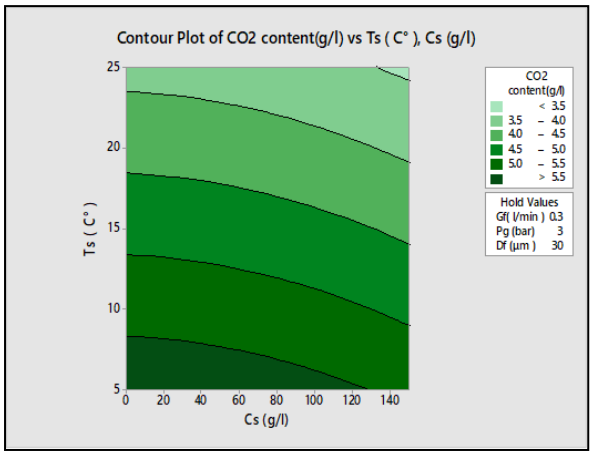

Figure 17 Contour of sucrose Concentration and Temperature

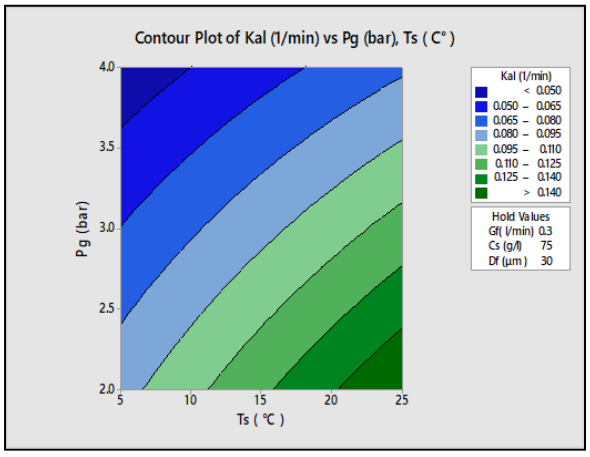

Figure 18 Contour plots Pressure and Temperature

According to Figure 20, which depicts the KLa of CO_2 present about the pressure and the concentration of sucrose, the KLa of CO_2 present is highest when the pressure is the lowest and the sucrose concentration is the midst value.

The KLa of CO_2 that is present can be shown to be a function of both the temperature and the flow rate of the gas in Figure 21. The KLa of CO_2 that is present can be seen to be at its highest when the temperature is the highest and the gas flow rate is the highest.

According to Figure 22, which depicts the KLa of CO_2 present about the gas flow rate and the concentration of sucrose, the KLa of CO_2 present is highest when the gas flow rate is the highest and the sucrose concentration is the midst value.

The KLa of CO_2 that is present can be shown to be a function of both the temperature and the sucrose concentration in Figure 23. The KLa of CO_2 that is present can be seen to be at its highest when the temperature is the highest and the sucrose concentration is the midst value.

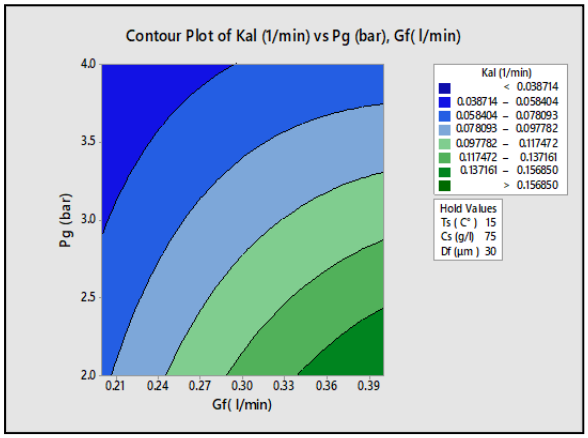

Figure 19 Contour plots Pressure and Gas flow rate

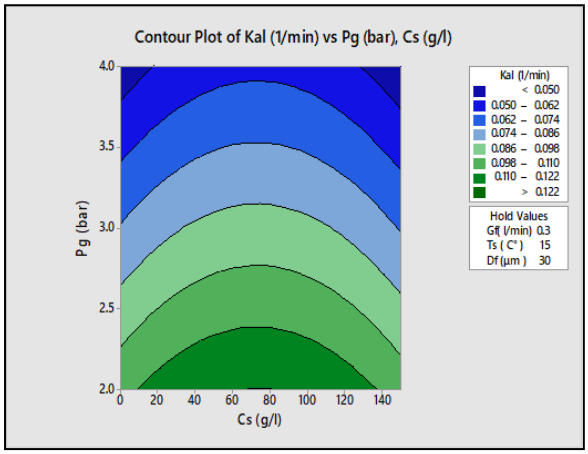

Figure 20 Contour plots Pressure and sucrose Concentration

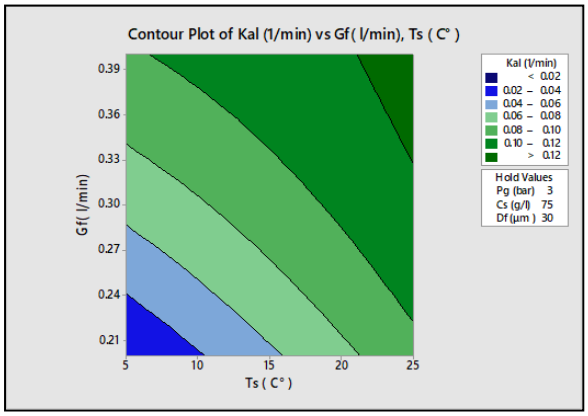

Figure 21 contour plots Temperature and Gas flow rate

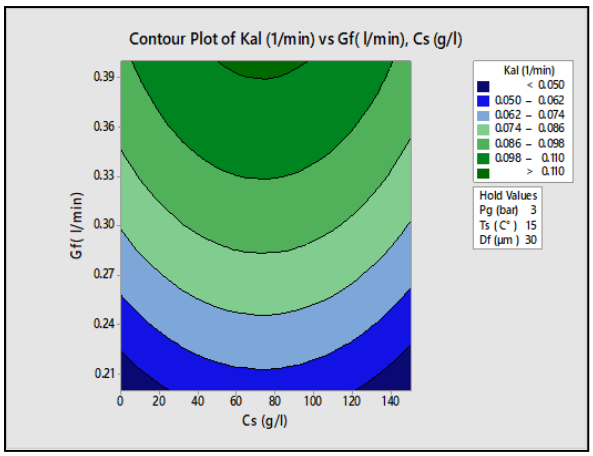

Figure 22 Contour plots of Gas flow rate and sucrose Concentration

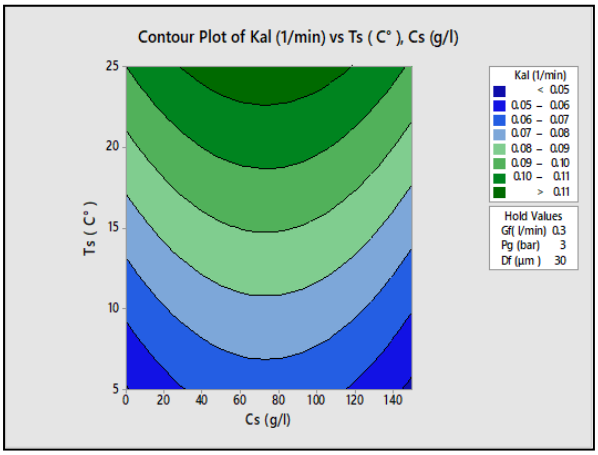

Figure 23 Contour plots of Gas flow rate and sucrose Concentration

4.4 Process Optimization

A high concentration of carbon dioxide (CO_2) and (KLa) is essential for effective implementation in the CO_2 absorption process when utilizing a sweetener solution for practical applications and Table 6 show the optimal conditions. The primary objective of this study was to determine the optimal conditions for maximizing the content and quality of CO_2 in a sucrose solution. Employing a response surface methodology (RSM) based on Box-Behnken design (BBD) allowed for this. Numerical optimization through the utilization of the desirability function was employed to select the desired values for various operating variables, including pressure, temperature, sucrose concentration, gas flow rate, and diameter of the pore diffuser. These desired values were chosen within a specified range. The responses, including the content and KLa of CO_2, were defined as "maximize" to identify the optimal conditions that would yield the desired responses [40, 41].

Table 6 ANOVA results for the RSM-BBD model of CO_2 content

Responses	Maximum	Pg	Ts	Gf	Cs	Df
		bar	°C	L/min	g/L	µm
Content CO_2	8.3456 (g/L)	4	5	0.4	0	0.5
KLa	0.1801 1/min)	2	25	0.4	72.72	0.5
Content CO_2 and KLa	6.125 (g/L) 0.1041(1/min)	2.83	5	0.4	65.14	0.5

5.0 CONCLUSION

Experimental data were used to fit a second-order polynomial model, which is the most prevalent model employed in RSM to determine the optimal conditions. A decrease in CO_2 content was observed with increasing temperatures, higher concentrations of sucrose, and smaller diffuser pore diameters. In contrast, an increase in CO_2 content was observed with increasing pressure and smaller diffuser pore diameters. A decrease in KLa was observed with increasing pressure and large diffuser pore diameters, while an increase in KLa was observed with increasing temperature and gas flow rate. The highest possible value of KLa was observed around the midpoint of the concentration range. Experimental results for achieving a high CO_2 content of 8.3456 g/L were 4 bars, a gas flow rate of 0.4 L/min, a sucrose aqueous solution with a concentration of 0 g/L, an absorption temperature of 5 °C, and a diffuser pore width of 0.5 µm. The optimal conditions for achieving a high KLa of 0.1801 (L/min) were 2 bar, a gas flow rate of 0.4 L/min, a sucrose concentration of 72.72 g/L, an absorption temperature of 25 °C, and a diffuser pore width of 0.5 µm.

Acknowledgments

Thanks, and appreciation to the employees of the chemical engineering department at the University of Baghdad, as well as the employees of the Ministry of Industry and Minerals _ Mansur factory, for their invaluable assistance and resources in making possible this research. Their knowledge and direction were crucial to our success

Conflicts of Interest

The author(s) declare(s) that there is no conflict of interest regarding the publication of this paper.

References

[1] Sujan, A., Vyas, R. K., Singh, K. 2018. Estimation of Liquid-side Mass Transfer Coefficient and Liquid Film Thickness in a Bubble Column using Single Spherical Bubble Model. *Asia-Pacific J Chem Eng*. 13(2): e2178.

[2] Devakumar, D., Saravanan, K., Kannadasan, T. *et al.* 2010. Mass Transfer Coefficient Studies in Bubble Column Reactor. *Mod. Appl. Sci.* 4(7): 65.
[3] Akita, K., Yoshida, F. 1974. Bubble Size, Interfacial Area, and Liquid-phase Mass Transfer Coefficient in Bubble Columns. *Ind Eng Chem Process Des. Dev*. 13(1): 84-91.
[4] Hikita, H., Asai, S., Tanigawa, K., *et al*. 1981. The Volumetric Liquid-phase Mass Transfer Coefficient in Bubble Columns. *Chem Eng J Elsevier.* 22(1): 61-69.
[5] Hammer, H. 1984. New Subfunctions on Hydrodynamics, Heat and Mass Transfer for Gas/Liquid and Gas/Liquid/Solid Chemical and Biochemical Reactors. *Front. Chem. Reac. Eng.* 464-74.
[6] Abe, S., Okawa, H., Hosokawa, S., *et al.* 2008. Dissolution of a Carbon Dioxide Bubble in a Vertical Pipe. *J. Fluid Sci. Technol.* 3(5): 667-77.
[7] Calderbank, P. H., Lochiel, A. C. 1964. Mass transfer Coefficients, Velocities and Shapes of Carbon Dioxide Bubbles in Free Rise through Distilled Water. *Chemical Engineering Science*. 19(7): 485–503. Doi: http://dx.doi.org/10.1016/0009-2509(64)85075-2.
[8] Al-mashhadani, M. K. H., Wilkinson, S. J., Zimmerman, W. B. 2016. Carbon Dioxide Rich Microbubble Acceleration of Biogas Production in Anaerobic Digestion. *Chem Eng Sci*. 156: 24-35. Doi: http://dx.doi.org/10.1016/j.ces.2016.09.011.
[9] Mahmood, R. S., Alsarayreh, A. A., Abbas, A. S. 2023. Measurement and Analysis of Bubble Size Distribution in the Electrochemical Stirred Tank Reactor. *Iraqi J. Chem. Pet. Eng.* 24(1): 27-31.
[10] Waisi, B. I., Majeed, J. T., Majeed, N. S. 2021. Carbon Dioxide Capture using Nonwoven Activated Carbon Nanofiber. *IOP Conference Series: Earth and Environmental Science 2021*. IOP Publishing.
[11] Majeed, N. S., Majeed, J. T. 2017. Study the Performance of Nanozeolite NaA on CO_2 Gas Uptake. *Iraqi J. Chem. Pet. Eng.* 18(2): 57-67.
[12] Teramoto, M., Tai, S., Nishii, K., *et al.* 1974. Effects of Pressure on Liquid-phase Mass Transfer Coefficients. *Chem. Eng. J.* 8(3): 223-26.
[13] Alvarez, E., Correa, J. M., Navaza, J. M., *et al.* 2001. Theoretical Prediction of the Mass Transfer Coefficients in Bubble Columns Operating in Churn-turbulent Flow Regime. Study in Newtonian and non-Newtonian Fluids under Different Operation Conditions. *Heat Mass Transf.* 37(4-5): 343-50.
[14] Zhu, D., Fang, M., Zhong, L., *et al.* 2011. Semi-batch Experimental Study on CO_2 Absorption Characteristic of Aqueous Ammonia. *Energy Procedia*. 4: 156-63.
[15] Alvarez, E., Cancela, M. A., Navaza, J. M., *et al.* 2002. Mass Transfer Coefficients in Batch and Continuous Regime in a Bubble Column. *Proc. Intl. Conference on Distillation and Absorption (Baden-Baden, Germany 2002.*
[16] Cho, H. J., Choi, J. 2019. Calculation of the Mass Transfer Coefficient for the Dissolution of Multiple Carbon Dioxide Bubbles in Sea Water under Varying Conditions. *J Mar Sci Eng.* 7(12). Doi: http://dx.doi.org/10.3390/JMSE7120457.
[17] Álvarez, E., Sanjurjo, B., Cancela, A., *et al.* 2000. Mass Transfer and Influence of Physical Properties of Solutions in a Bubble Column. Chem. Eng. Res. Des. 78(6): 889-93.
[18] Wilkinson, P. M., Haringa, H., Dierendonck, L. L. Van. 1994. Mass Transfer and Bubble Size in a Bubble Column under Pressure. *Chem. Eng. Scil.* 49(9): 1417-27.
[19] Idogawa, K., Ikeda, K., Fukuda, T., *et al.* 1987. Formation and Flow of Gas Bubbles in a Pressurized Bubble Column with a Single Orifice or Nozzle Gas Distributor. *Chem. Eng. Commun.* 59(1-6): 201-12.
[20] Al-Hemiri, A. A., Salih, S. A. 2007. Prediction of Mass Transfer Coefficient in Bubble Column using Artificial Neural Network. *Journal of Engineering.*
[21] Rastegar, Z., Ghaemi, A. 2022. CO_2 Absorption into Potassium Hydroxide Aqueous Solution: Experimental and Modeling. *Heat Mass Transf.* 58(3): 365-81.
[22] Al-Hemiri, A. A., Selman, M. D. 2011. Estimation of Mass Transfer Coefficients in a Packed Distillation Column using Batch Mode. *Iraqi J Chem Pet Eng.* 12(1): 13-21.
[23] Dhuyool, A. W., Shakir, I. K. 2023. Carbon Dioxide Capturing via a Randomly Packed Bed Scrubber Using Primary and Poly Amine Absorbents. *J Ecol Eng.* 24(11): 14-29. Doi: http://dx.doi.org/10.12911/22998993/170205.
[24] Atiya, Z. Y. 2012. Estimation of Volumetric Mass Transfer Coefficient in Bioreactor. *Al-Khwarizmi Eng. J.* 8(3): 75-80.
[25] Olsen, J. E., Dunnebier, D., Davies, E., *et al*. 2017. Mass Transfer between Bubbles and Seawater. *Chem Eng Sci Elsevier.* 161: 308-15.
[26] Myers, R. H., Montgomery, D. C., Vining, G. G, *et al.* 2004. Response Surface Methodology: A Retrospective and Literature Survey. *J Qual Technol*. 36(1): 53.
[27] Baş, D., Boyacı, İ. H. 2007. Modeling and Optimization I: Usability of Response Surface Methodology. *J. Food Eng.* 78(3): 836-45.
[28] Amiri, M., Shahhosseini, S., Ghaemi, A. 2017. Optimization of CO_2 Capture Process from Simulated Flue Gas by Dry Regenerable Alkali Metal Carbonate-based Adsorbent using Response Surface Methodology. *Energy & Fuels.* 5: 5286-96.
[29] Mohammad, N. K., Ghaemi, A., Tahvildari, K. 2019. Hydroxide Modified Activated Alumina as an Adsorbent for CO_2 Adsorption: Experimental and Modeling. *Int. J. Greenh Gas Control.* 88: 24-37.
[30] Saeidi, M., Ghaemi, A., Tahvildari, K., *et al.* 2018. Exploiting Response Surface Methodology (RSM) as a Novel Approach for the Optimization of Carbon Dioxide Adsorption by Dry Sodium Hydroxide. *J. Chinese Chem. Soc.* 65(12): 1465-75.
[31] Almoslh, A., Alobaid, F., Heinze, C., *et al.* 2020. Influence of Pressure on Gas/liquid Interfacial Area in a Tray Column. *Appl. Sci.* 10(13): 4617.
[32] Wang, B., Lu, X., Tao, S., *et al.* 2021. Preparation and Properties of CO_2 Micro-nanobubble Water based on Response Surface Methodology. *Appl. Sci.* 11(24): 11638.
[33] Descoins, C., Mathlouthi, M., Moual, M. Le, *et al.* 2006. Carbonation Monitoring of Beverage in a Laboratory Scale Unit with on-line Measurement of Dissolved CO_2. *Food Chem*. 95(4): 541-53.
[34] Diamond, L. W., Akinfiev, N. N. 2003. Solubility of CO_2 in Water from− 1.5 to 100 C and from 0.1 to 100 MPa: Evaluation of Literature Data and Thermodynamic Modelling. *Fluid Phase Equilib*. 208(1-2): 265-90.
[35] Tokumura, M., Baba, M., Kawase, Y. 2007. Dynamic Modeling and Simulation of Absorption of Carbon Dioxide into Seawater. *Chem. Eng. Sci.* 62(24): 7305-11.
[36] Martínez, I., Casas, P. A. 2012. Simple Model for CO_2 Absorption in a Bubbling Water Column. *Brazilian J. Chem. Eng. SciELO Brasil.* 29: 107-11.
[37] Rumpf, B., Xia, J., Maurer, G. 1998. Solubility of Carbon Dioxide in Aqueous Solutions Containing Acetic Acid or Sodium Hydroxide in the Temperature Range from 313 to 433 K and at Total Pressures up to 10 MPa. *Ind Eng Chem Res.* 37(5): 2012-19.
[38] Yincheng, G., Zhenqi, N., Wenyi, L. 2011. Comparison of Removal Efficiencies of Carbon Dioxide between Aqueous Ammonia and NaOH Solution in a Fine Spray Column. *Energy Procedia*. 4: 512-18.
[39] Yoo, M., Han, S-J., Wee, J-H. 2013. Carbon Dioxide Capture Capacity of Sodium Hydroxide Aqueous Solution. *J. Environ. Manage.* 114: 512-19.
[40] Mourabet, M., Rhilassi, A. El, Boujaady, H. El, *et al.* 2017. Use of Response Surface Methodology for Optimization of Fluoride Adsorption in an Aqueous Solution by Brushite. *Arab J. Chem*. 10: S3292-302.
[41] Bezerra, M. A., Santelli, R. E., Oliveira, E. P., *et al*. 2008. Response Surface Methodology (RSM) as a Tool for Optimization in Analytical Chemistry. *Talanta.* 76(5): 965-77.